SCANNING ELECTRON MICROSCOPY OF CLAYS AND CLAY MINERALS

B. F. BOHOR and RANDALL E. HUGHES

Illinois State Geological Survey, Natural Resources Building, Urbana, Ill. 61801

Abstract – The scanning electron microscope (SEM) proves to be ideally suited for studying the configuration, texture, and fabric of clay samples. Growth mechanics of crystalline units – interpenetration and interlocking of crystallites, crystal habits, twinning, helical growth, and topotaxis – also are uniquely revealed by the SEM.

Authigenic kaolins make up the bulk of the examples because their larger crystallite size, better crystallinity, and open texture make them more suited to examination by the SEM than most other clay mineral types.

INTRODUCTION

THE SCANNING electron microscope (SEM) is uniquely suited for studying clays because it affords a magnified, three-dimensional view of the unmodified (natural) clay surface with great depth of focus. The only sample preparation necessary for clays is a thin metallic coating, applied in a vacuum evaporator, which serves to prevent a build-up of electrons on the surfaces by conducting away static electricity. With the conventional transmission electron microscope (TEM), the surfaces of clay particles cannot be directly observed, and only by an involved and time-consuming procedure of replication can they be viewed at all.

A simple description of the principles of operation and performance of the SEM is excerpted below from the sales brochure of the Advanced Metals Research Corporation (1969, p. 2):

Resolution is of the order of 200Å and the useful magnification, up to about 50.000 ×, is in a convenient range lying between that of the light optical microscope and the transmission electron microscope. Most important, however, the depth of focus one obtains is of the order of tens of microns. This means that a fairly rough surface, such as produced by a metal fracture or exhibited by a small biological specimen, will remain entirely in focus at high magnifications. The micrograph obtained is similar in appearance to that of the reflection light microscope but, again, with much better resolution and depth of focus.

The principle of operation of the SEM is by now quite familiar. An electron optical column, containing electromagnetic lenses, demagnifies an electron source in order to focus a fine beam of electrons on the specimen surface. This beam is scanned across the specimen surface in a rectangular raster in synchronism with the spot of a cathode ray tube. The signal resulting from interaction of the beam with the specimen is collected by a suitable electron detector and used to modulate the CRT brightness. In most applications it is the low-energy secondary electrons which are thus used to form a picture of the specimen on the CRT face.

With the installation 2 years ago of a Stereoscan SEM (Cambridge Electronic Instruments Ltd.,Cambridge, England) in the Central Facility for Electron Microscopes at the University of Illinois, we began a study to see what this new tool would reveal about clays and clay minerals. It immediately became apparent that certain clay minerals were more suited to examination than others because of their greater size, better crystallinity, and distinctive morphology. Some of the best results under the SEM were obtained from authigenic varieties of kaolinite. Because of this, and because of numerous projects at the Illinois State Geological Survey involving kaolinite, the majority of our observations have been on this mineral. However, we have included micrographs of many of the other common clay minerals to demonstrate the observations that can be made on any clay material with the SEM.

Many papers have been published on the applications of the SEM, but only a few are concerned with clay minerals. Borst and Keller (1969) studied many of the API Project 49 reference clays. Gillot (1969) and many other authors have included a few SEM micrographs of clays, but the instrument has not been extensively applied in clay mineralogical research. Perhaps this is because of the legacy of fine micrographs produced from replicas on the

49

TEM by Bates and Comer (1955), Beutelspacher and Van der Marel (1968), and others too numerous to mention. We hope to show, however, that the SEM, because of its unique operation and performance, can bring new dimensions to our understanding of clay minerals.

TECHNIQUE

Sample preparation is unusually simple for such a sophisticated instrument, and this greatly enhances its usefulness and applicability. Sample size is limited to about one-half cubic inch (1 in. $\times$ 1 in. $\times \frac{1}{2}$ in.) in the instrument used, but newer models can accommodate specimens more than four times this volume.

Samples can be mounted by a variety of methods. Powders can be sprinkled directly on an adhesive mounting medium, such as Duco cement, double stick tape, or silver or chrome paint, or they can be sprayed on a metallic foil subsequently attached to the specimen stub; rock fragments may be directly mounted on the stub. Our mounting stubs (Engis Equipment Co., Morton Grove, Ill.) are aluminum discs 12 mm in dia. with a shank on the back. If small pieces of material are used, as many as six or eight samples can be accommodated on each stub, thereby avoiding time-consuming changing of specimens.

One of our first studies with the SEM was made during the development of a method of spray-drying clay minerals to reduce their preferred orientation in X-ray powder diffraction analysis (Hughes and Bohor, 1970). The method can be described simply as spraying a dilute clay suspension through a heater to form spherical aggregates of clay minerals. In theory, the clay platelets should be arranged with their basal surfaces tangential to the spherical water droplets formed during spraying and remain oriented in this fashion when the water is driven off in the heater. The resulting powder, composed mainly of spheres, can then be packed in the usual powder diffraction holders and any preferred basal (or other anisotropic) orientation should be eliminated. Clay minerals are thoroughly randomized by spray-drying, and therefore details of individual particle morphologies are more easily seen when some clays are prepared as sprayed powders for SEM examination.

Because clay materials are nonconductors of electrons, the samples must be coated with a thin layer of conductive material to prevent charge build-up. To accomplish this, a gold-palladium coating about 50–100 Angstroms (Å) thick is deposited on the samples by evaporation under high vacuum. This thin coating in no way modifies the surface details or hinders viewing, because the resolution of commercial SEM instruments is not less than 200 Å

even under optimum conditions. To get a continuous conductive coating over the usually rough and porous surface of a clay sample, the metallic layer is deposited in two operations and at two different angles on a rotating stage. Thus the effective solid angle of incidence of the applied metallic layer approaches 90°, and it effectively coats all the available surfaces.

Because clay minerals are quite hygroscopic, the stub-mounted samples must be over-dried overnight before the coating is applied, and they should be kept dry after being coated to prevent rupture of the conductive layer and to shorten the microscope's pump-down time. To meet these requirements, the stub shanks are inserted into the base of a cork, which fits into a small glass or plastic vial. A small amount of dessicant is put into the vial, and, when the cork with its attached stub is inserted, an effective portable micro-dessicator results. The sample stubs can then be stored indefinitely in these vials and transported to the microscope in the optimum dry condition.

OBSERVED FEATURES OF CLAYS AND CLAY MINERALS

Certain features of clays and clay minerals are more readily observed on the SEM than by other conventional means. These features include those involving the surface and 3-dimensional aspects of clay minerals, such as the morphology (configuration) of samples, fabric (particle boundary relationships), texture (overall particle arrangements), and growth mechanics of crystals and crystallites. Examples of the latter feature shown here include the variations in layer (packet) thickness, crystal habit, topotaxis (crystallographic control of the development of later diagenetic minerals by pre-existing minerals), twinning and spiral growth (helical growth about a central axis).

Configuration

Figures 1(a), 1(b), 2(a), and 2(b) show how the SEM can solve the problem of determining the morphology (configuration) of a spray-dried powder. Figure 1(a) is a highly magnified view of a natural rock sample of kaolinite from Anna, Illinois. White (1958) determined by particle-size and X-ray analyses that this clay was composed of unusually fine particles (more than 85 per cent of them less than 0.5μ) of rather poorly crystallized kaolinite, and Fig. 1(a) confirms these determinations directly. Even the large plates of the clay appear to be composed of much smaller platelets. Figure 1(b) shows a spray-dried sample of this same Anna kaolinite, illustrating the typical spherical aggregates artificially formed during spraying and the
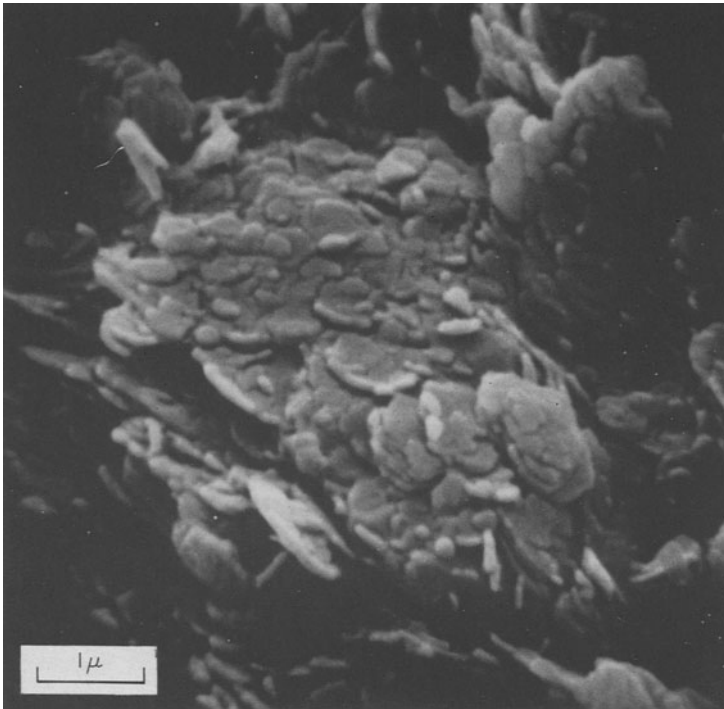
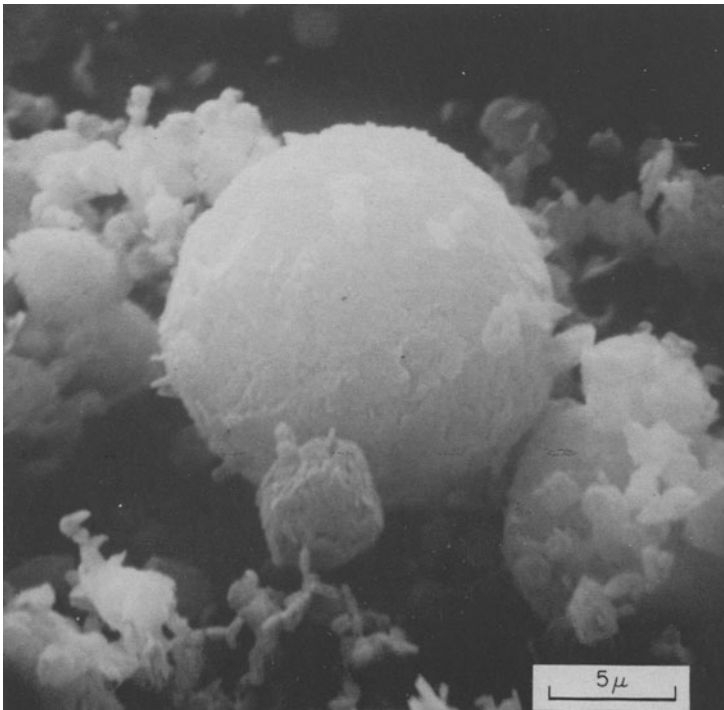Fig. 1(a). Rock sample of kaolinite from near Anna, Union Co., Illinois (Cretaceous or Tertiary).

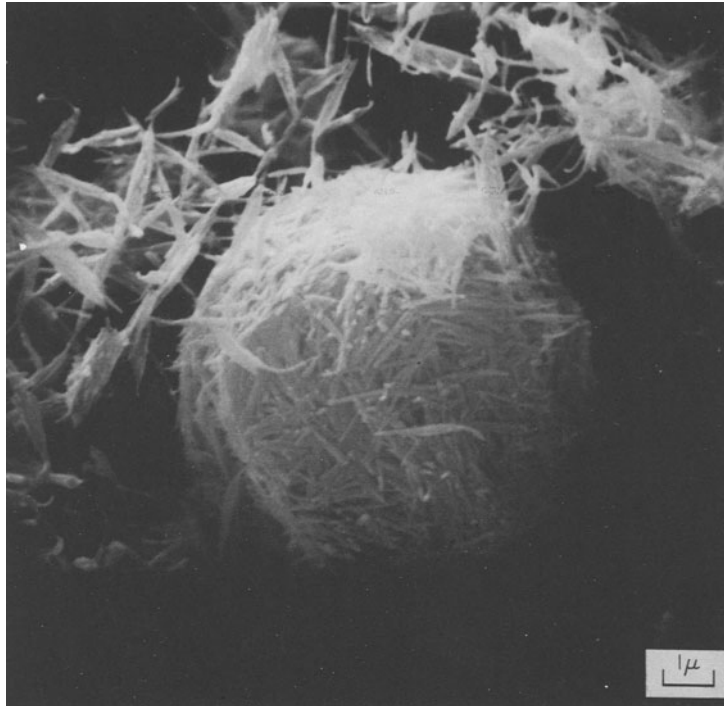Fig. 1(b). Spray-dried kaolinite from near Anna, Union Co., Illinois.

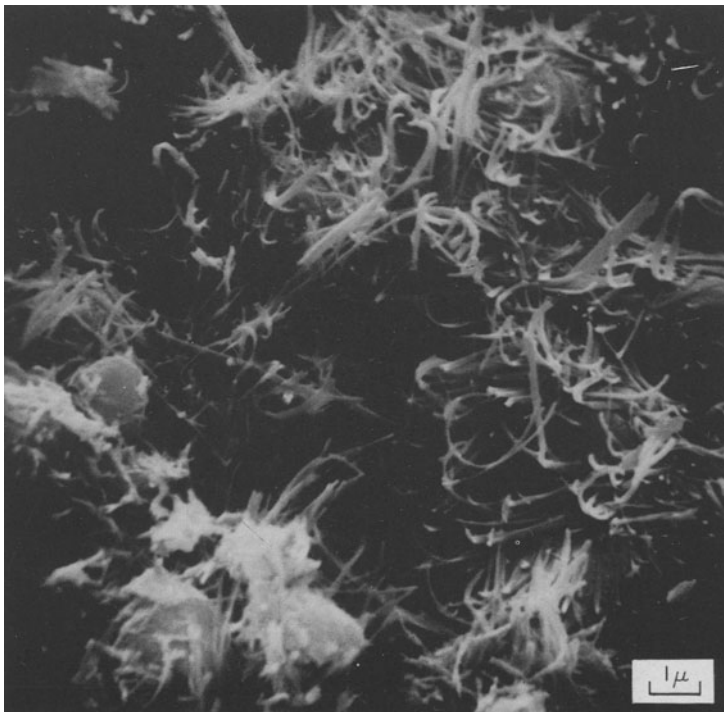Fig. 2(a). Spray-dried attapulgite from Yucatan, Mexico.

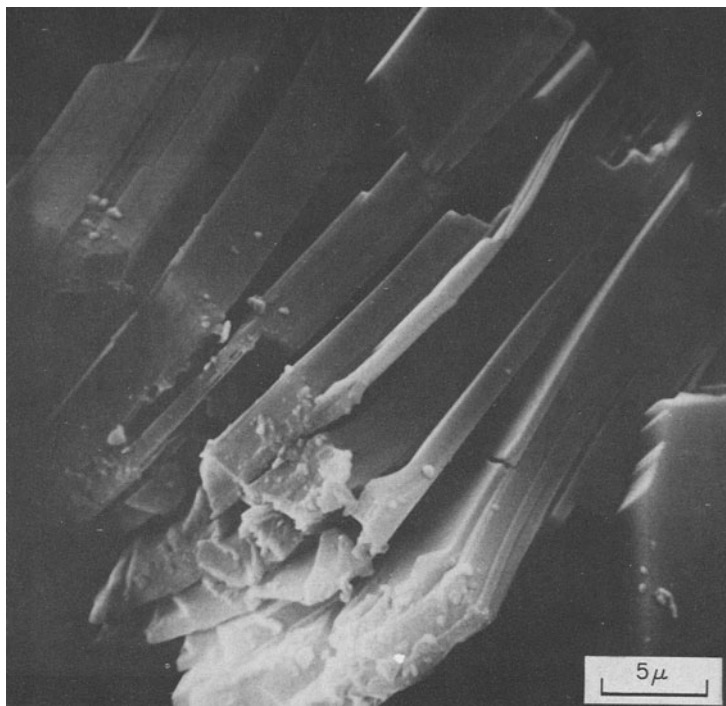Fig. 2(b). Rock sample of attapulgite from Yucatan, Mexico (Tertiary).

Fig. 3(a). Authigenic kaolinite from the interior of a claystone concretion in the Francis Creek Member (shale) of the Carbondale Formation, Grundy Co., Illinois (Pennsylvanian).

Fig. 3(b). Authigenic cleat kaolinite from the Herrin (No. 6) Coal Member, Carbondale Formation, Sangamon Co., Illinois (Pennsylvanian).

Fig. 4(a). Cross section of cleat containing kaolinite (right) and pyrite (left) from the Herrin (No. 6) Coal Member, Carbondale Formation, Sangamon Co., Illinois (Pennsylvanian).
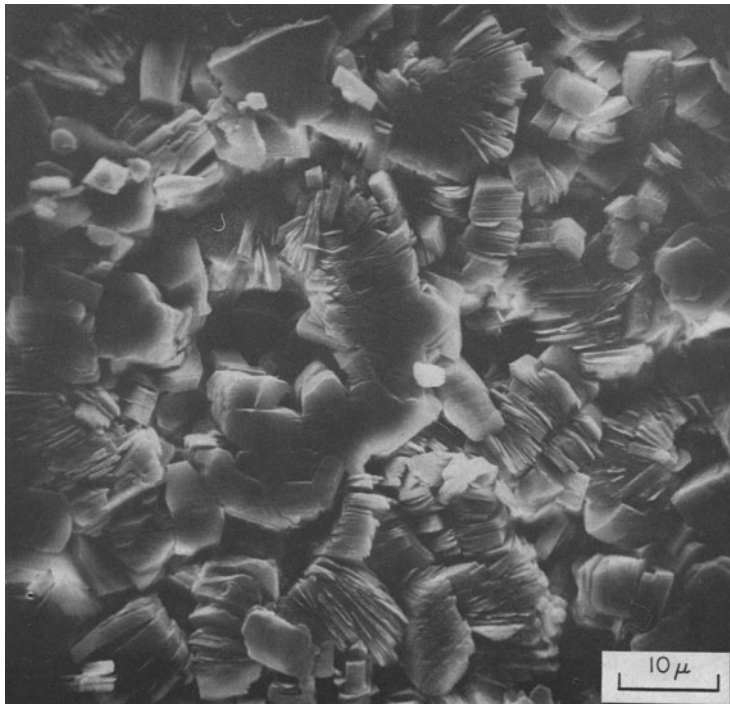

Fig. 4(b). Normal view of kaolinitic cleat surface; Herrin (No. 6) Coal Member, Sangamon Co., Illinois (Pennsylvanian).

Fig. 5(a). Normal view of pyrite cleat surface with kaolinite packets growing through; Herrin (No. 6) Coal Member, Carbondale Formation, Sangamon Co., Illinois (Pennsylvanian).
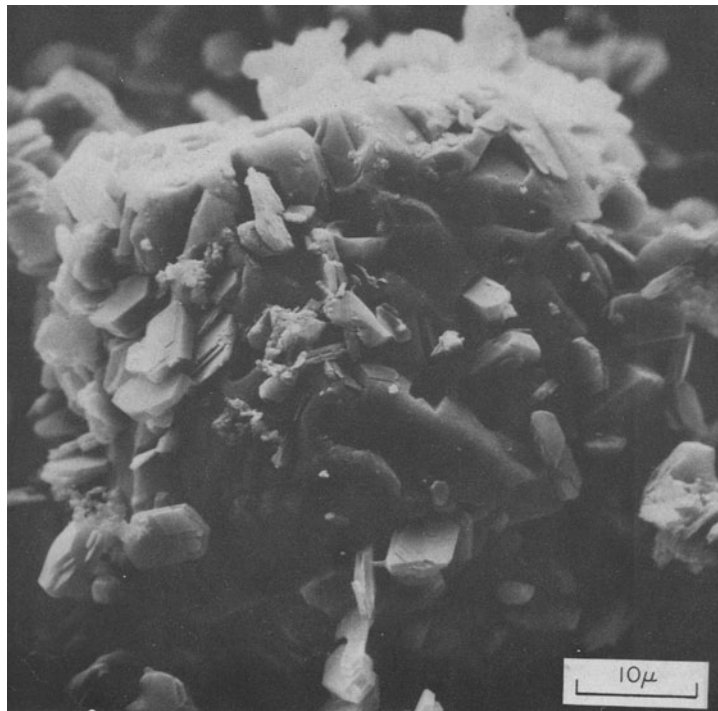

Fig. 5(b). Authigenic kaolinite growing in quartz crystal; geode from the Warsaw Formation, Hamilton Co., Illinois (Mississippian).
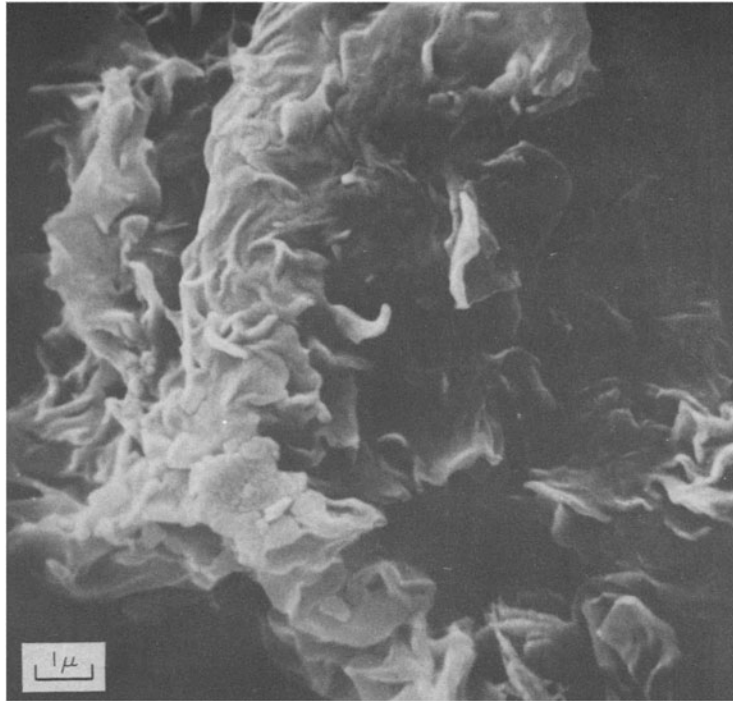
Fig. 6(a). Rock sample of bentonite from Clay Spur, Wyoming (A.P.I. No. 26) (Cretaceous).
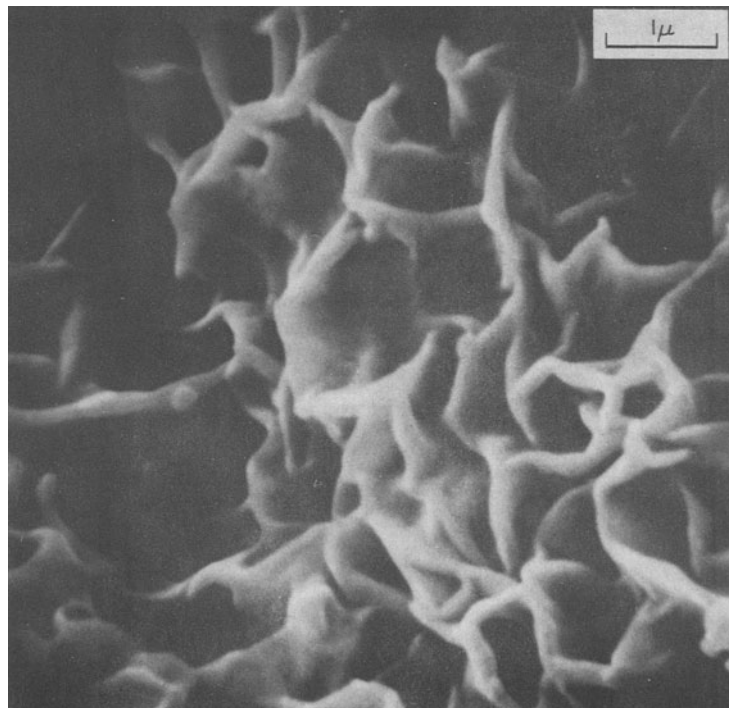

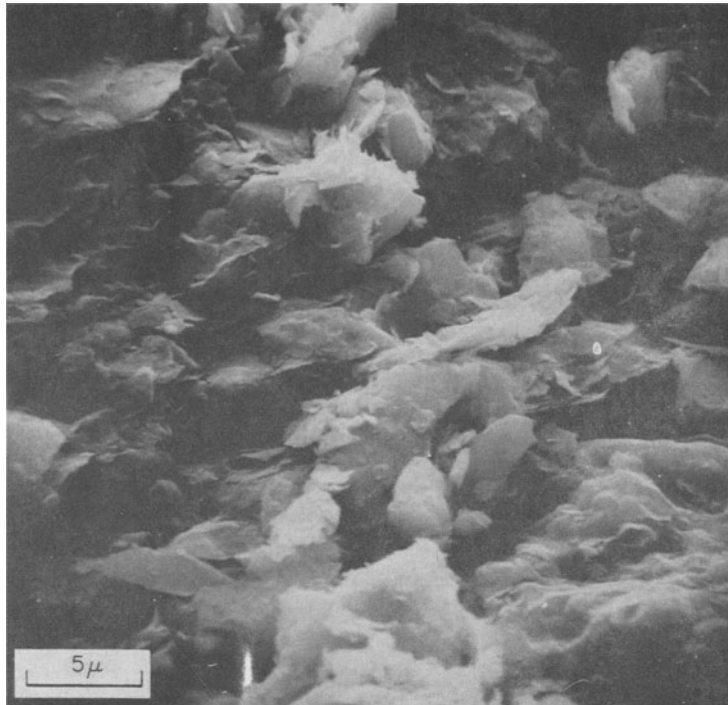Fig. 6(b). Rock sample of Wyoming bentonite (A.P.I. No. 26).

Fig. 7(a). Illitic clay from the "Blue Band," a clay seam (split) in the Herrin (No. 6) Coal Member, Carbondale Formation, Sangamon Co., Illinois (Pennsylvanian).
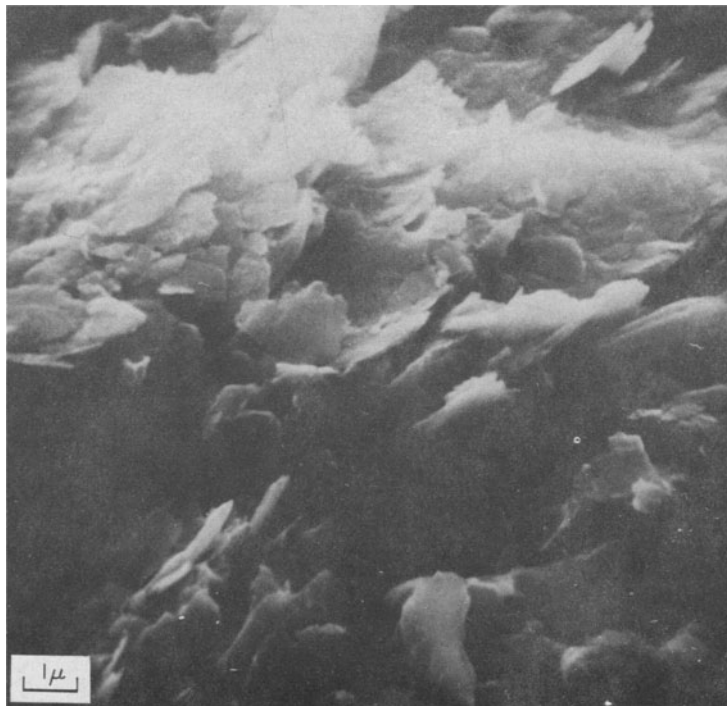

Fig. 7(b). Underclay from beneath the Colchester (No. 2) Coal Member, Carbondale Formation, Mercer Co., Illinois (Pennsylvanian).
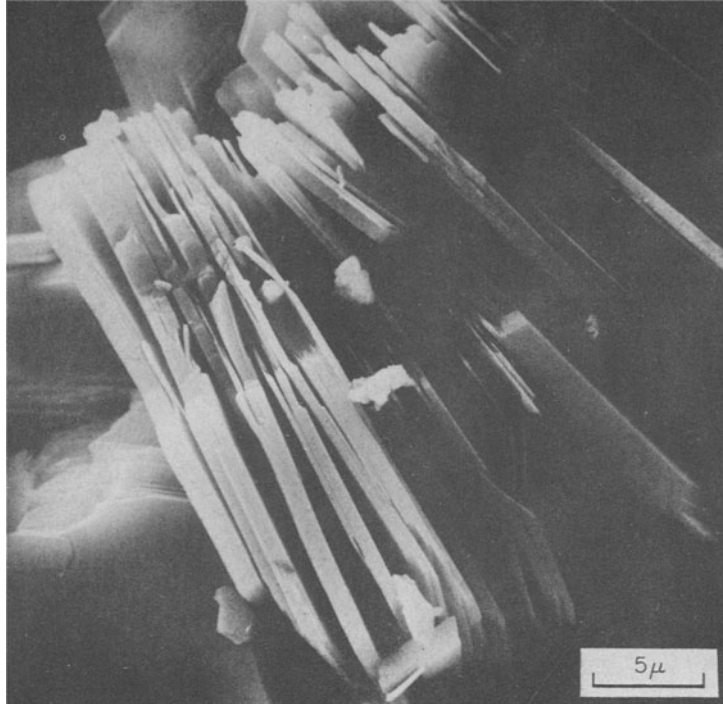
Fig. 8(a). Edge view of authigenic kaolinite packet; from concretion in the Francis Creek Member of the Carbondale Formation, Grundy Co., Illinois **(Pennsylvanian).**

Fig. 8(b). Side view of thick, obscurely laminated packet of authigenic kaolinite from a concretion: Francis Creek Member, Carbondale Formation, Grundy Co., Illinois (Pennsylvanian).

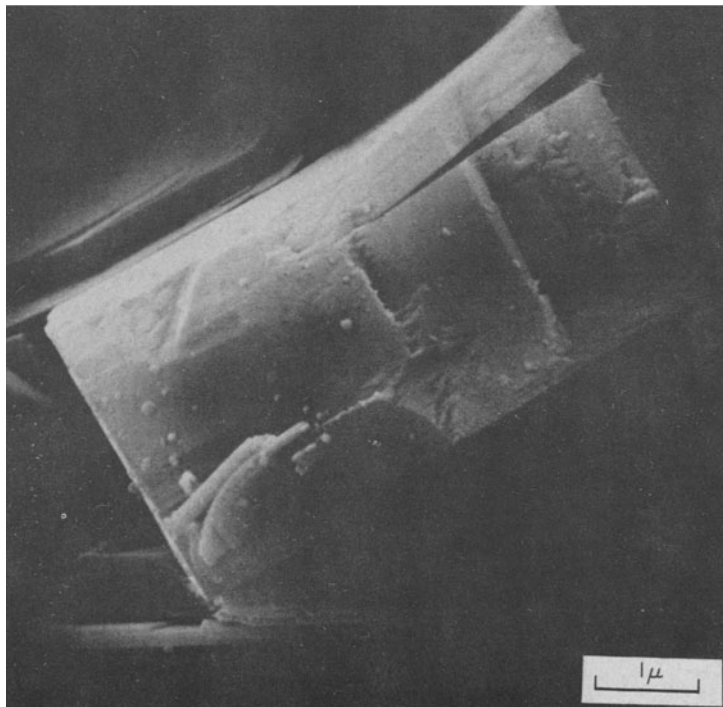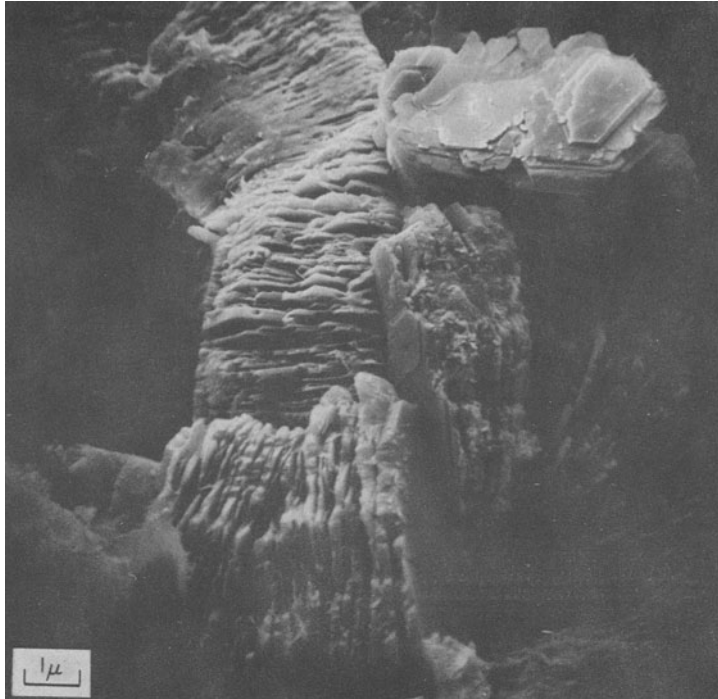Fig. 9(a). Authigenic kaolinite vermicules in pores of a sandstone; St. Peter Formation, La Salle Co., Illinois (Ordovician).
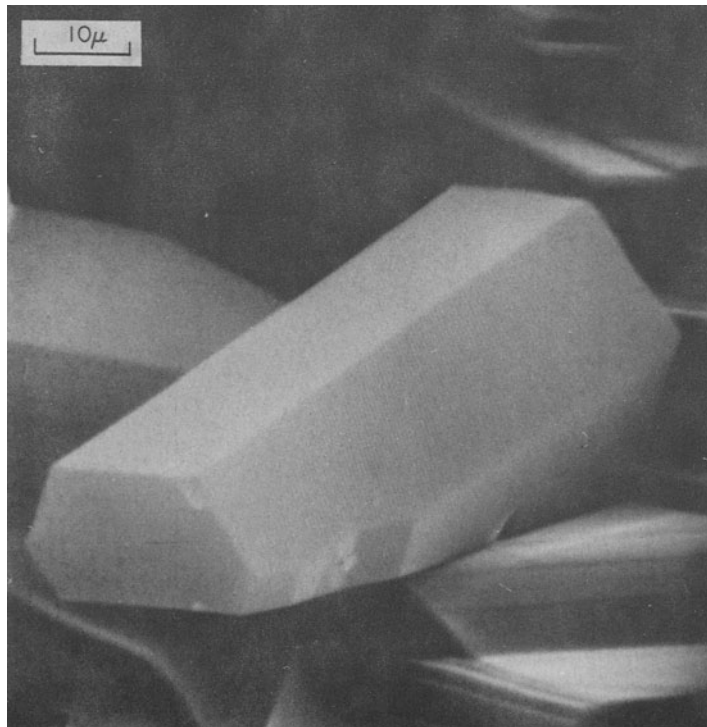
Fig. 9(b). Single crystal of dickite from a limestone in the Lansing-Kansas City Group, Wilson Co., Kansas (Pennsylvanian).
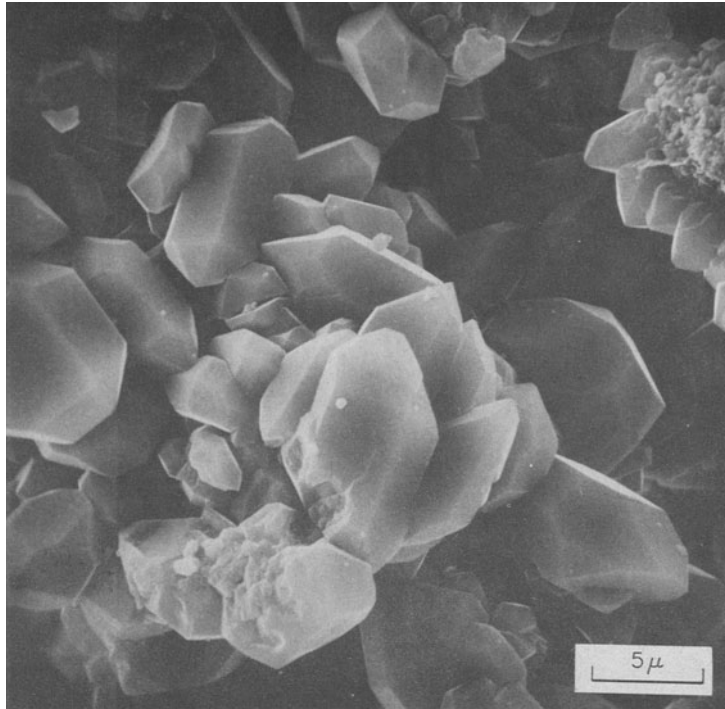
Fig. 10(a). Quartz microcrystals in a replaced fossil; Clear Creek Formation, Union Co., Illinois (Devonian).
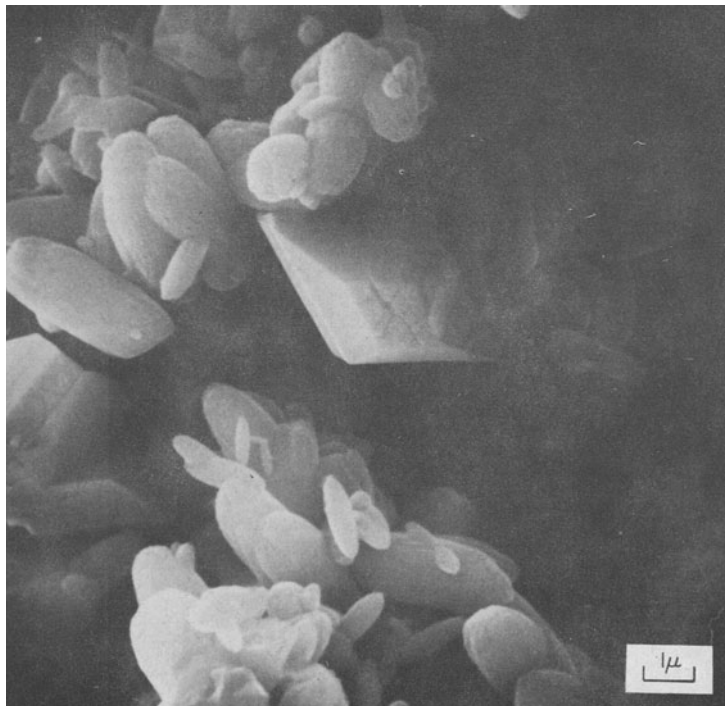
Fig. 10(b). Unusual crystalline phases in white bauxite from Montenegro, Yugoslavia.
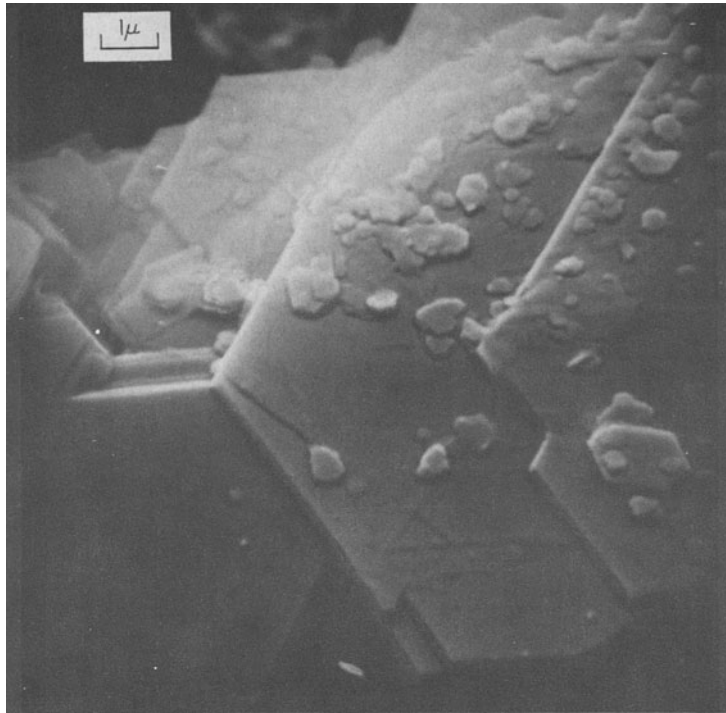
Fig. 11(a). Secondary illite laths on authigenic kaolinite plates: St. Peter Formation, La Salle Co., Illinois (Ordovician).
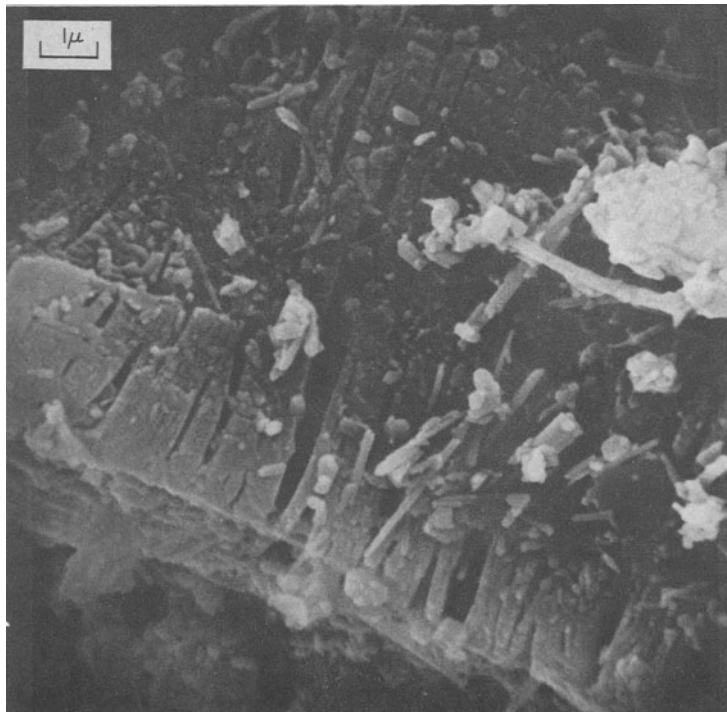
Fig. 11(b). Laths of kaolin mineral (probably halloysite) developing from weathering of feldspar crystal: Spruce Pine, North Carolina (A.P.I. No. 51).
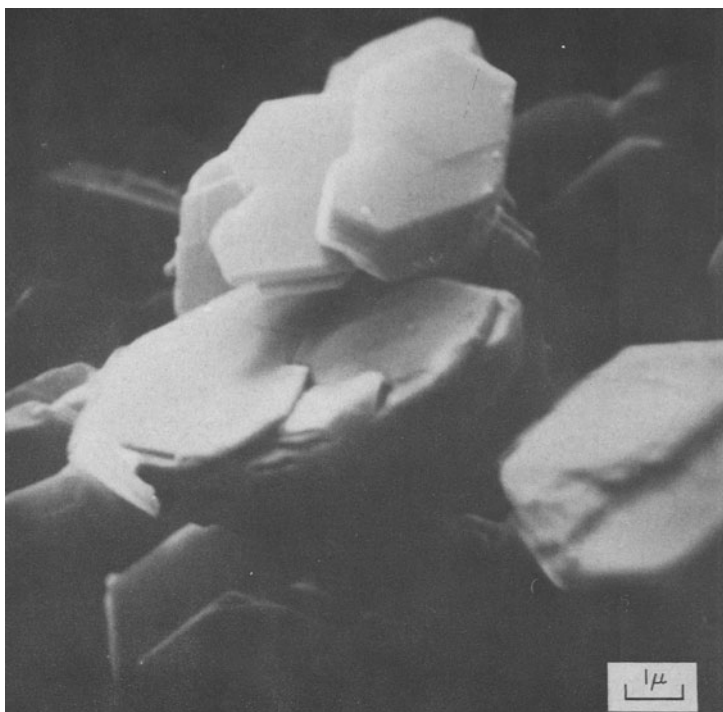
Fig. 12(a). Spiral growth and twinning of authigenic kaolinite from a geode; **Warsaw Formation**, Hamilton Co., Illinois (Mississippian).
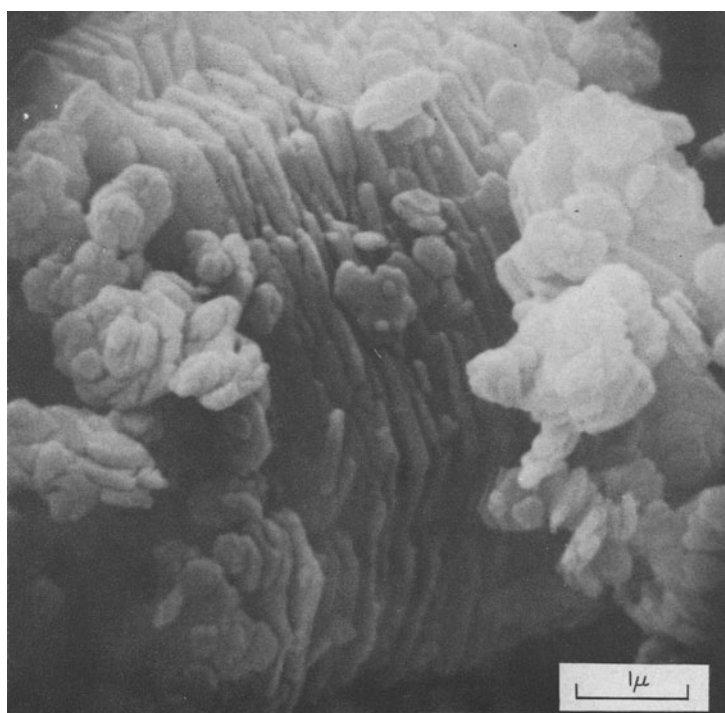
Fig. 12(b). Composite vermicule in kaolinite from Georgia (Eocene).
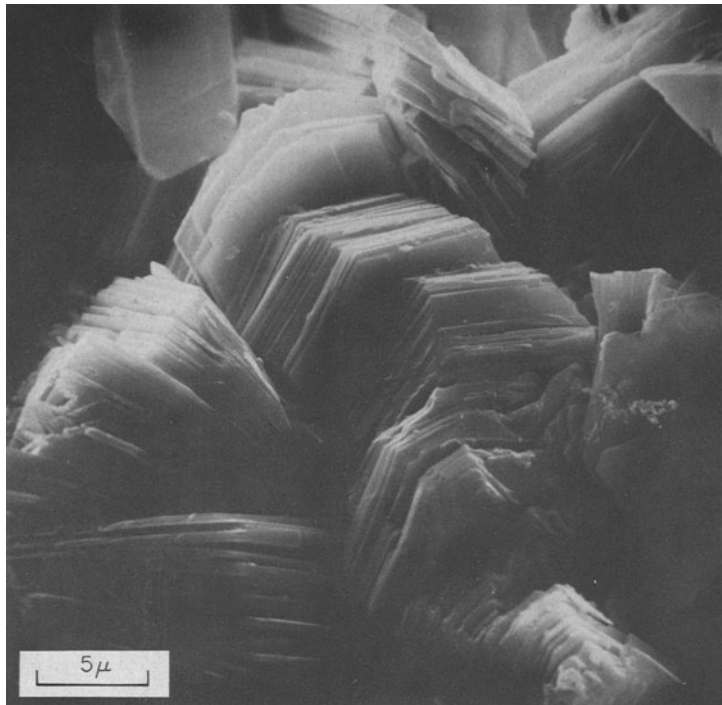
Fig. 13(a). Uniform vermicular stacks of dickite from Utah.
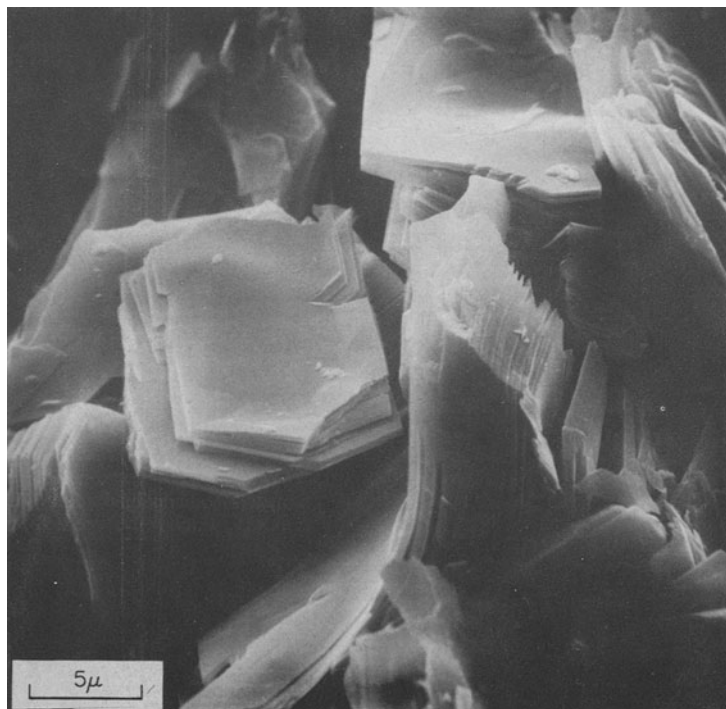
Fig. 13(b). Twinned and bent crystallites of dickite from Utah.
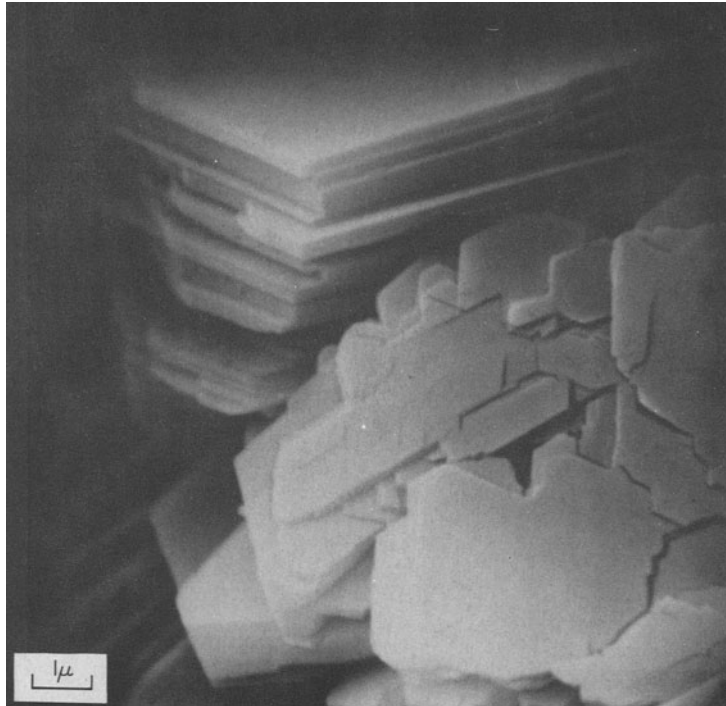
Fig. 14(a). Mosaic of small kaolinite crystals forming larger crystallites in cleat; Herrin (No. 6) Coal Member, Carbondale Formation, Sangamon Co., Illinois (Pennsylvanian).

Fig. 14(b). Cantilevered stacking sequence of platelets in kaolinite stack; concretion in Francis Creek Member, Carbondale Formation, Grundy Co., Illinois (Pennsylvanian).

tangential arrangement of the clay mineral platelets around the circumference of the sphere. Obviously, the particles arranged themselves in this fashion because of the surface tension in the original suspension droplet formed by the nebulizer, and they retained this arrangement while the water was being driven off in transit through the drying tube.

Figure 2(a), a view of natural rock attapulgite from Mexico, is atypical in that its needle-like crystallites shown here are usually compacted into massive, featureless blocks. This micrograph does show the morphology of the crystallites quite well, however; notice the longitudinal bending of the thinner crystallites that have at least one free end, and the lath-like aggregate of crystallites extending upward from the surface in the center right portion of the micrograph. Apparently, fracturing during sample preparation disrupted and lifted a small area of the crystallite packets.

Figure 2(b) is the same Mexican attapulgite after ultrasonic dispersion and spray drying. The spherical aggregate with the typical "ball of yarn" appearance results from tangential adhesion of the attapulgite crystallites. The bundles of crystallites in the background are free powder or "dust" generated by aggregates too large to accrete tangentially to water droplets. This "dust" is a typical component of spray-dried powders, and its ratio to the spherical aggregates varies directly with the particle size of the sprayed material for any given range of droplet sizes (sprayer characteristics).

Attapulgite is a difficult mineral to prepare properly and examine in the SEM in its natural (rock) state because it is finely acicular and has a high water sorption capacity. An area such as a broken edge where the individual crystallites are exposed and noncontiguous is usually selected for viewing but, because of the extremely irregular nature of the surface at these points, a continuous metallic coating almost never exists and heavy charging develops. Also, when the electron beam is focused down to the high magnifications required to view these individual crystallites adequately, the concentrated heat of the beam drives some of the channel water out of the mineral, resulting in abrupt sample movements and contamination of the microscope. The magnitude of these problems is greatly reduced, however, when the sample is prepared by spray drying. The surfaces of the spheres are much smoother and more easily coated with the vaporized metal, and the crystallites arranged tangentially on the spherical surface are individually quite well displayed (Fig. 2b). Because much less material is exposed to the electron beam and the mounting foil acts as a heat sink, sample degassing (water expulsion) is almost eliminated and sample movement and microscope contamination are reduced.

Fabric

The SEM is unique in its ability to reveal interparticle relations, such as interlocking and interpenetration features, aggregate arrangement (face-to-face vs. edge-face) and shrinkage (drying) features. Figures 3(a) and (b) illustrate interlocking in authigenic kaolinites. Figure 3(a) shows the typical "stepped" appearance of this fabric feature in the lower right of the micrograph. The sample is kaolinite within a concretion. Figure 3(b) also shows interlocking and interpenetration of kaolinite layer packets at the right of the micrograph. This sample is cleat kaolinite (authigenic kaolinite forming along dessication or shrinkage cracks) from the vitrain layers in coal. The thick packet in the center of the micrograph displays evidence of twinning, as shown by the nonparallelism of the platelet edges along the upper surface of the crystal compared with the edges exposed at the middle of the micrograph. Similar interlocking of crystals and packets occurs in flint clay and partly accounts for its difficulty of dispersion, as well as that of cleat and concretion kaolinites.

Texture

On a larger scale, interlocking can occur where two types of materials grow into contact. Figure 4(a) is a cross section of the contact between pyrite on the left and kaolinite on the right in a cleat (vertical dessication crack or parting) filling in an Illinois coal. Pyrite often occurs between the coal surface and the main vein filling of kaolinite in cleats, and the irregular contact between these two shows the strong penetration of kaolinite into the pyrite. In contrast, Fig. 4(b) shows the surface of a kaolinite-filled cleat that originally was in direct contact with the coal with no intervening pyrite layer. The termination (sealing) of packets against the coal by both basal and prism surfaces is flat. The two micrographs clearly show why cleat kaolinite can be separated easily from coal, but only with difficulty from any associated pyrite.

Further evidence of intergrowth and penetration textures due to corrosion are shown by Figs. 5(a, b). Another instance of the growth of kaolinite packets through a cleat pyrite layer in a coal is shown in Fig. 5(a). The environment is the same as that in Fig. 4(a), but the view is now perpendicular to the extended cleat surface of the pyrite. The blocky, stepped texture of the pyrite can be seen clearly in this micrograph. Solutions that somewhat preceded deposition of the kaolinite seem to have produced holes in the pyrite layer by corrosive action in which the clay then grew. Some post-corrosion, prismatic pyrite crystals appear to have grown on the walls of these holes. Figure 5(b) reveals a slightly different intergrowth texture involving

authigenic kaolinite and quartz formed in a geode. Here the quartz-kaolinite contacts are more sharply defined and more parallel, indicating a closer control on corrosion of the quartz by the later-forming kaolinite crystallites themselves.

Another aspect of texture is shown by the next two sets of figures (Figs. 6a, b, 7a, b). The first micrograph (Fig. 6a) shows the typical surface appearance of a clay largely composed of smectite — a bentonite from Wyoming. This crinkly, ridged, honeycomb-like texture (shown in a closer view in Fig. 6(b)) is characteristic of the smectite group and probably develops from shrinkage of the expandable clay minerals as they dry. The polygonal pattern of this texture resembles dessication mud cracks and other dewatering features. Individual crystal platelets are almost invisible in the smectites because they are small and dispersed, leaving an impression of cohesive thin films composing the basic textural units of these clays.

Between the filmy texture of the smectites and the aggregates of rather thick, stubby plates in the kaolinites (Fig. 1a), is the texture of illitic clays, such as that found in a shale split (the so-called "Blue Band") in an Illinois coal shown in Fig. 7(a). Several small ovoid pods, characteristic of illitic clay minerals found in some underclays, are shown on the left in the micrograph, along with the wavy surfaces of the clay flakes. The detrital illites are generally composed of thin anhedral plates and aggregates. Figure 7(b) shows an underclay from Illinois and again exhibits the typical claystone texture, plus some good examples of individual illite platelets, especially at the left in the micrograph.

Growth mechanics

Details of crystal growth mechanics in clays, such as layering (packet thicknesses), crystal habit, topotaxis, twinning, and spiral growth can be studied with the SEM if the clay mineral crystallites are large, well formed, and of a fairly open texture. Of all the clays we have studied, these criteria are best fulfilled by the authigenic kaolins, which provide most of our examples of these growth features. Authigenic kaolinites collected in Illinois include samples from a concretion, from the interstitial pores of a sandstone, and from the interior of a geode. One sample of a kaolinite from Georgia (courtesy of Georgia Kaolin Company) is also included. Other authigenic kaolin minerals included are samples of dickite from southeastern Kansas and Utah, an example of "halloysite" from North Carolina, and a white bauxite sample from Yugoslavia (courtesy of Professor Olga Sarc-Lahodny, University of Zagreb).

Packet thicknesses vary in authigenic kaolinite.

Figures 8(a), (b) depict this variability in a sample of kaolinite from a concretion in a shale from Illinois. In Fig. 8(a), the side view of a stack shows a majority of relatively thin packets of nearly equal thickness. However, closer examination of these packets, especially along broken surfaces, reveals that they are composed of many thinner platelets. An accurate count of the number of platelets making up each packet cannot be made because of the limits imposed by the resolving power of the microscope. In contrast to these thin packets, Fig. 8(b) shows an extremely thick packet from this same concretion. A parting is beginning to develop in the upper quarter, and the lower third of the packet seems to be twinned, as no parallel lamellae edges are visible and the plates seem to meet the overlying packet with angular unconformity. There is probably some factor controlling the thickness of packets, but we have not yet identified it from these micrographs.

Examples of crystal forms and habits are shown in Figs. 9(a), (b), 10(a), (b). Authigenic kaolinite and dickite usually crystallize as stacks of packets, whose length (stacking on the (001) basal surfaces) sometimes exceeds their diameter by several orders. These are the familiar vermicules, or worms, of the tonsteins and other clays. Figure 9(a) shows vermicular kaolinite growing in pores of a sandstone from an outcrop in Illinois. Similar vermicular growth by extended basal stacking was displayed in the cleat sample (Fig. 5a). However, Figure 9(b) shows a crystal form of the kaolin group quite different from the usual stacked buildups of two-dimensional platelets. This unusual morphology was found in dickite from a limestone in southeastern Kansas. It is pseudohexagonal, which is compatible with the monoclinic nature of dickite. It is certainly not quartz, because of its crystal habit and its lack of basal pinacoids. When it is compared with the authigenic quartz crystals from southern Illinois in Fig. 10(a), the difference in crystal morphology is obvious. The tiny pseudohexagonal prism of Fig. 9(b) is apparently either an unusual crystallization of dickite or is some other form of hydrous alumina. As X-ray diffraction analysis showed only dickite, quartz, and calcite present in this sample, the unidentified mineral must be dickite. This case of questionable identity is an example of the potential value of a microprobe accessory, for the problem could have been solved in short order had such a unit been attached to our SEM.

Some other interesting crystal forms that might be found in high alumina clays are shown in Fig. 10(b), a sample of white bauxite from Yugoslavia. The rounded crystallites similar in appearance to grains of rice are probably boehmite, the major

bauxite mineral in this sample, and the diamond-shaped crystal near the center may be prismatic gibbsite. These crystal habits are only rarely observed in this sample, the bulk being composed of massive, anhedral aluminates. The well formed crystals seemingly develop only in pores and other voids.

Some evidence for topotaxic clay mineral growth has been observed with the SEM. Figure 11(a) shows the surface of some well formed vermicules of authigenic kaolinite in a sandstone. Imposed on these planar surfaces are very thin, long laths, often overlying one another at 60° angles. These lath-like crystallites are interpreted as authigenic illite, possibly generated by a chemical groundwater reversal during the Pleistocene Epoch. The illite laths are secondary to the kaolinite, because several of the faint laths drape over the edge of one kaolinite platelet and continue onto the surface of the underlying platelet (right-hand side of the micrograph). Such topotaxic growth control (120° angles of growth) exercised by the pseudohexagonal kaolinite on secondary illite also was clearly shown by Rex (1966), and the reasons for it are adequately explained in his paper.

Figure 11(b) is "halloysite" from Spruce Pine, North Caroline. The micrograph shows a feldspar grain weathering to a lath-like kaolin mineral, probably halloysite. The lath-shaped, rod-like crystals forming on the surface of this grain are only tentatively identified as halloysite, however, because in none of the many micrographs made of this clay, nor in the SEM pictures of this same material in Borst and Keller (1969), have any true open-ended tubes been clearly recognized. The originally stubby halloysite crystal laths may elongate by secondary growth on the ends of the prisms (or tubes) to form the slender rods characteristic of the Spruce Pine kaolin. TEM replicate micrographs of this material (Taggart *et al.*, 1955) usually show scrolled or spatulate tubes, unlike the laths shown here.

Twinning and spiral growth are fairly common in the authigenic kaolins, but finding clearly defined examples is rather difficult. Figure 12(a) is a rarity because it displays both these growth phenomena. The crystal packet at the top of the picture is twinned on $hk0$ where $h = k$, probably the most common type of twinning in kaolinite. The larger packet in the center shows the spiral growth mode. This latter phenomenon results in pseudohexagonal crystals that share common interior edges and extend helically in the c-direction to form the larger crystallites of kaolinite vermicules. Figure 12(b) illustrates this composite growth of kaolinite vermicules very well in a sample of Georgia kaolinite. This micrograph is an oblique view of a large vermicule with serrated edges that result from the

stacking of a large number of smaller, hexagonal platelets in columnar arrangement around a central axis. Similar serration or scalloping of vermicule edges can be seen in Figs. 5(a), 9(a). Serration seems to be characteristic of authigenic vermicular kaolinites. Authigenic dickite (Fig. 13a) does not usually show this serration. However, twinning is common in dickite, as is shown by the small crystals at the far right center of Fig. 13(a), and the lack of serration is probably due to a slightly different growth mode. Figure 13(b) shows a twinned crystal at the left center of the micrograph, with a large, bent sheaf of platelets just to the right and below it.

Further evidence of twinning, composite crystals, and spiral growth in authigenic kaolinite is given by Figs. 14(a), (b). The highly composite nature of large crystallites is shown by the grouping in the lower right of Fig. 14(a), a sample of cleat kaolinite from Illinois. In the concretion kaolinite of Fig. 14(b), interpenetration is exhibited at the lower left, while the stack of platelets in the upper center shows the "cantilever" structure that sometimes is caused by precession or eccentricity of the spiral growth axis. This cantilever effect is rather common in authigenic kaolinite and dickite.

SUMMARY AND CONCLUSIONS

The SEM has proved very useful for studying clay minerals. Its speed and ease of operation, high magnification, and great depth of focus make it uniquely suited to the study of very fine-grained materials and surfaces.

Past SEM work in clay mineralogy has been primarily concerned with the description of members of the various clay mineral groups. From our studies we conclude that the SEM is almost indispensable for the study of clay mineral configuration (size and shape), fabric (interpenetration), texture (intergrowth), and growth mechanics. In the latter category, such growth-related phenomena as layering, crystal habit, topotaxis, twinning, and spiral growth are clearly visible in samples of many of the larger, well crystallized clay minerals, such as the authigenic kaolinites.

Advances in technology should make the SEM even more useful for studying clay minerals. Particularly needed are increased resolution and built-in spectrographic (microprobe) capabilities.

Because we have clearly observed corrosive effects in nature, excellent information on the effects of artificial mechanical (abrasion) and artificial chemical (etching) treatments should be obtainable with the SEM. The high degree of form demonstrated for authigenic minerals in nature also suggests that further investigation of synthetic and artificial weathering products with the SEM would be profitable.

REFERENCES

Advanced Metals Research Corporation (1969) AMR High Resolution Scanning Electron Microscope, Model 900: Advanced Metals Research Corporation, Burlington, Mass.

Bates, T. F. and Comer, J. J. (1955) Electron microscopy of clays: *Clays and Clay Minerals* **3**, 1–25.

Beutelspacher, H. and Van der Marel, H. W. (1968) *Atlas of Electron Microscopy of Clay Minerals and Their Admixtures—A Picture Atlas* 333 p. Elsevier, Amsterdam.

Borst, R. L. and Keller, W. D. (1969) Scanning electron micrographs of API reference clay minerals and other selected samples: *Proc. Intern. Clay Conf. Tokyo* Vol. I, 871–901. Israel University Press, Jerusalem.

Gillot, J. E. (1969) Study of the fabric of fine-grained sediments with the scanning electron microscope: *J. Sediment. Petrol.* **39**, 90–105.

Hughes, R. E. and Bohor, B. F. (1970) Random clay powders prepared by spray drying: *Am. Mineralogist* **55**, No. 9–10, 1780–1786.

Rex, R. W. (1966) Authigenic kaolinite and mica as evidence for phase equilibria at low temperatures: *Clays and Clay Minerals* **13**, 95–104.

Taggart, M. S., Jr., Milligan, W. O. and Studer, H. P. (1955) Electron micrographic studies of clays: *Clays and Clay Minerals* **3**, 31–64. [*NAS-NRC Publ. 395*]

White, W. A. (1958) Water sorption properties of homoionic clay minerals: *Ill. State Geol. Surv. Rept. Invest. 208*.

Résumé—La microscope électronique à balayage (SEM) prouve qu'il est parfaitement adapté à l'étude de la configuration, de la texture et de la structure des prélèvements argileux. La mécanique de croissance des unités cristallines—interpénétration et inter-verrouillage des cristallites, constitution de cristal, entrelacement, croissance hélicoïdale et topotaxie—est également révélée d'une manière unique par le SEM.

Les kaolins authigéniques forment l'ensemble des exemples à cause de leur cristallite de plus grande taille, de leur meilleure cristallinité et de la texture ouverte qui les rend plus appropriés que les autres types de minéraux argileux, à l'examen par SEM.

Kurzreferat—Es wird festgestellt, dass sich das Abtastelektronenmikroskop (SEM) ideal für die Untersuchung des Gefüges, der Textur und der Struktur von Tonproben eignet. Die Wachstummechanik der gegenseitigen Eindringung kristalliner Einheiten und die Verknüpfung von Kristalliten, Kristallhabitus, Verzwillingung, schraubenförmiges Wachstum und Topotaxis werden ebenfalls auf einzigartige Weise durch SEM zum Vorschein gebracht.

Authigene Kaoline stellen den Hauptanteil der Proben dar weil ihre bedeutendere Kristallitgrösse, ihre bessere Kristallinität und offene Textur sie der Prüfung durch das SEM besser zugänglich machen als die meisten anderen Arten von Tonmineralen.

Резюме — Показано, что сканирующая электронная микроскопия представляет собой идеальный метод для изучения конфигурации, текстуры и структурно-морфологических характеристик образцов глин. Механизм роста кристаллитов, характер их прорастаний и срастаний, габитус кристаллов, двойникование, спиральный рост и топотаксия — все это наилучшим образом выявляется методом сканирующей электронной микроскопии.

Основную массу изученных автором образцов составили аутигенные каолиниты, которые, благодаря большим размерам кристаллитов, более высокой степени кристалличности и ясновыраженной текстуре, являются гораздо более пригодными для изучения методом сканирующей электронной микроскопии, чем другие глинистые минералы.